




Development and evaluation of an anti-candida cream based on silver nanoparticles

Antônio Auberson Martins Maciel^{1,2} · Francisco Afrânio Cunha^{1,2} · Tiago Melo Freire¹ · Fernando Lima de Menezes¹ · Lillian Maria Uchoa Dutra Fachine¹ · Janaina Sobreira Rocha¹ · Rita de Cássia Carvalho Barbosa² · Roxeane Teles Martins² · Maria da Conceição dos Santos Oliveira Cunha^{3,4} · Ralph Santos-Oliveira^{5,6} · Maria Veraci Oliveira Queiroz³ · Pierre Basílio Almeida Fachine¹ 

Received: 17 May 2023 / Accepted: 17 September 2023 / Published online: 4 October 2023
© King Abdulaziz City for Science and Technology 2023

Abstract

The ineffectiveness of azole drugs in treating Vulvovaginal Candidiasis (VVC) and Recurrent Vulvovaginal Candidiasis (RVVC) due to antifungal resistance of non-*albicans* *Candida* has led to the investigation of inorganic nanoparticles with biological activity. Silver nanoparticles (AgNPs) are important in nanomedicine and have been used in various products and technologies. This study aimed to develop a vaginal cream and assess its in vitro antimicrobial activity against *Candida parapsilosis* strains, specifically focusing on the synergy between AgNPs and miconazole. AgNPs were synthesized using glucose as a reducing agent and sodium dodecyl sulfate (SDS) as a stabilizer in varying amounts (0.50, 0.25, and 0.10 g). The AgNPs were characterized using UV–Visible (UV–Vis) and Fourier-Transform Infrared (FT-IR) spectroscopies, X-Ray Diffraction (XRD), Dynamic Light Scattering (DLS), Scanning Electron Microscopy (SEM), and Energy Dispersive X-Ray Analysis (EDX). Fifty strains of *Candida parapsilosis* were used to evaluate the synergistic activity. AgNPs synthesized with 0.5 g SDS had an average size of 77.58 nm and a zeta potential of -49.2 mV, while AgNPs with 0.25 g showed 91.22 nm and -47.2 mV, respectively. AgNPs stabilized with 0.1 g of SDS were not effective. When combined with miconazole, AgNPs exhibited significant antifungal activity, resulting in an average increase of 80% in inhibition zones. The cream developed in this study, containing half the miconazole concentration of commercially available medication, demonstrated larger inhibition zones compared to the commercial samples.

Keywords Silver nanoparticles · *Candida* · Miconazole · Antifungal activity

Introduction

Vulvovaginal Candidiasis (VVC) is one of the most common gynecologic problems, affecting around 75% of women worldwide (Willems et al. 2020). In addition, approximately 9% of VVC cases evolve into a more aggressive form known as Recurrent Vulvovaginal Candidiasis (RVVC), wherein more than three episodes are observed within one year. VVC and RVVC are caused by an overgrowth of the *Candida* species in the mucous membrane of the lower genital system, leading to inflammation of the vulva, vulvar itching, and abnormal vaginal discharge (Lírio et al. 2022; Rosati et al. 2020). In general, patients with these symptoms suffer from low self-esteem and frustration, significantly affecting their social and sexual life and that of their partners (Moshfeghy

et al. 2020). *Candida albicans* is the responsive agent of more than 90% of VVC cases. However, other non-*albicans* *Candida*, such as *Candida glabrata*, *Candida parapsilosis*, *Candida tropicalis*, and *Candida krusei*, have also been frequently reported and, in some places, can exceed 50% of the cases (Willems et al. 2020).

The treatment of VVC is usually performed with vaginal creams containing imidazoles, triazoles or nystatin drugs for up to 14 days (Cianci et al. 2020; Farr et al. 2021). While RVVC requires a more prolonged antifungal therapy using mainly imidazole drugs for up to 6 months (Lírio et al. 2022). However, using a specific group of medications, such as azole drugs, for extended periods can trigger side effects, including a metallic taste in the mouth, headache and dizziness, and an increment in antifungal resistance, complicating the treatment (Johnson 2021; Parsapour et al. 2021; Willems et al. 2020). Indeed, it has been shown that

Extended author information available on the last page of the article

both *C. parapsilosis* and *Albicans* have strains that are less susceptible to azole treatment, limiting the choice of empirical antifungal therapy (Dhasarathan et al. 2021; Tóth et al. 2019). Therefore, the search for new drugs or azole formulations that present high activity with low side effects has been carried out by researchers worldwide (Sobel and Nyirjesy 2021).

To develop more efficient drugs against the proliferation of yeasts, researchers have used inorganic nanoparticles that provided excellent results minimizing the colonizing effects of *Candida* species (Mare et al. 2021; Tauseef et al. 2022). Indeed, metallic nanoparticles such as silver and gold have good biocompatibility and antifungal properties. Silver is a metal with a lower cost than gold, making it attractive for developing a new antifungal drug. In addition, it is known that silver nanoparticles with a diameter of less than 100 nm can interact with the membranes of yeast cells, leading to their destabilization and later the formation of pores and cytoplasm leakage (Szerencsés et al. 2020). However, it has been reported that AgNPs synthesized by plants have a moderate inhibitory effect against *Candida* spp. (Al-Baharani et al. 2018). In contrast, when AgNPs are stabilized using sodium dodecyl sulfate (SDS), the synergetic effect improves the fungicidal activity due to better accessibility of the AgNPs into the cell (Panáček et al. 2009).

In this sense, some studies explore the synergistic effect of colloidal-AgNPs in association with traditional drugs to reduce their amount during the treatment of candidiasis, minimizing the side effects and overcoming *Candida* spp. antifungal resistance (Devi and Joshi 2012; Szerencsés et al. 2020; Vazquez-Muñoz et al. 2014). For example, the action of fluconazole and itraconazole have been enhanced in the presence of AgNPs (Guerra et al. 2020; Singh et al. 2013). Therefore, this work aims to present the development of an antifungal vaginal cream containing AgNPs and miconazole. Additionally, in vitro tests were conducted to evaluate the efficacy of the product against 50 strains of *Candida parapsilosis*.

Materials and methods

Materials

Glucose (Dinâmica, São Paulo, Brazil, purity > 98.5%), silver nitrate (Dinâmica, São Paulo, Brazil, purity > 99%), sodium dodecyl sulfate (SDS) (Synth, São Paulo, Brazil, purity > 98.5%), Mueller–Hinton agar (Himedia, India), methylene blue (Dinâmica, São Paulo, Brazil, purity > 98.5%), miconazole (Sigma, USA), and carbopol (Dinâmica, São Paulo, Brazil). All the reagents were used without further purification.

For the experiment, 50 strains of *Candida parapsilosis*—the most common in fungal infections in Ceará, Brazil—were selected. These strains were isolated from blood samples between 2007 and 2013. Moreover, they are part of the Yeast Collection of the Yeast Microbiology Laboratory of the Department of Clinical and Toxicological Analyses of the School of Pharmacy, Dentistry and Nursing of the Federal University of Ceará (LML/DACT/FFOE/UFC) (Menezes et al. 2012).

Synthesis and purification of AgNPs

Three colloidal suspensions containing silver nanoparticles (AgNPs) were prepared with varying amounts of the stabilizing/capping agent (SDS). Briefly, 5.55×10^{-3} mol of glucose and 3.46×10^{-4} mol (0.10 g) of SDS were solubilized in 500 mL of 5.0×10^{-3} mol L⁻¹ AgNO₃ solution. To catalyze the reaction, 1.0 mL of 0.2 mol L⁻¹ NaOH was added, and the resulting solution was heated up to 50 °C under vigorous stirring. After 30 min, the system was allowed to cool to room temperature. Next, the suspension was centrifugated at 10,000 RPM (revolutions per minute) for 20 min, washed three times with distilled water, and the AgNPs were suspended in distilled water. The resulting sample was labeled as AgNPs-0.10. The other two suspensions were prepared using 8.66×10^{-4} mol (0.25 g) and 1.73×10^{-3} mol (0.50 g) of SDS and labeled AgNPs-0.25 and AgNPs-0.50, respectively. Finally, all the samples were stored at 4 °C until further use.

Anti-candida cream formulation

The anti-candida cream was prepared using the active ingredients at 10% (w/w) concentrations for AgNPs-0.50 and 1% (w/w) miconazole (half of the commonly utilized concentration of this drug). The choice of the AgNPs-0.50 was based mainly on their antifungal activity when associated with miconazole and colloidal stability. Then, after choosing the nanoparticles, carbopol was used as a vehicle, as its bioadhesive properties are well documented, facilitating the retention of the cream in the vagina (Salah et al. 2018). The final product presented a light color, a pleasing texture, and no grittiness, as shown in Fig. 5a.

Cultivation of the strains

For the experiment, 50 strains of *Candida parapsilosis* were previously stored in distilled water, inoculated on potato agar (Himedia Mumbai, India) and incubated at 35 °C/24–48 h. Then, they were seeded on CHROMagar Candida (Himedia Mumbai, India) to assess purity. The process was done three times to ensure purity. The identification was carried out by micromorphology on rice agar supplemented with

tween 80 by verifying germ tube production, fermentation, and assimilation of carbohydrates.

Characterization of the AgNPs

Initially, the synthesized AgNPs were characterized by measuring the absorbance. It is well-known that AgNPs have a plasmon band in the UV–Vis spectrum. The presence of AgNPs in the solutions was evaluated through UV–Vis spectrophotometry in the 300–700 nm wavelength range on a Thermo Scientific GENESYS™ 10 s spectrophotometer. The FT-IR analyses were performed on a Perkin-Elmer FT-IR Spectrum ONE spectrophotometer in the 4000–400 cm^{-1} range with a resolution of 4 cm^{-1} . Previously to the measurement, the samples were dried and mixed with potassium bromide (KBr) to obtain powder and then pressed in disk format. The diffractogram patterns were obtained using PAN analytical X-pert Pro MRD (Amsterdam, Netherlands). The pure AgNPs sample was placed on a glass support measuring 2.5×2.5 cm, and the diffractogram was collected using $K\alpha$ radiation of Cu and Ni with a negative potential of 40 kV and 30 mA. The scanning angle (2θ) ranged from 20° to 80° with a step of 0.033° per second. The Dynamic Light Scattering (DLS) analysis was performed to verify the average hydrodynamic size and polydispersity index (PDI) of the AgNPs by light scattering. Colloidal stability was evaluated by measuring zeta potential. The device used was the Nanozetasizer (Malvern, United States). Morphological evaluation of the AgNPs was performed by scanning electron microscopy (SEM). This process was done on the Quanta FEG 450 with EDS/EBSD and cooling/heating stage.

Association between miconazole and AgNPs

The association evaluation method was the disc diffusion protocol in Mueller–Hinton agar supplemented with 2% glucose and 0.05% methylene blue (Hashemi et al. 2022). Briefly, the strains were seeded on each plate, and five types of discs (22 mm) were produced using filter papers. Thus, the miconazole discs were prepared by adding 25 μL of miconazole solution with a concentration of 1 $\mu\text{g}/\mu\text{L}$. The discs of AgNPs-0.25 and AgNPs-0.50 were prepared by adding 25 μL of AgNPs-0.25 and AgNPs-0.50 solution, respectively. To prepare the disc of the silver nanoparticles associated with miconazole, 10 mg of miconazole were solubilized in 10 mL of each solution of AgNPs-0.25 and AgNPs-0.50. Then, the discs were prepared by adding 25 μL of each sample to the paper filter. The AgNPs-0.10 sample was not used because it did not show absorbance compatible with AgNPs (Fig. 2a). After the production of the discs, they were placed in the oven at 35°C for 48 h for water evaporation. The discs

were stored at -8°C until the use time, which was always less than 5 days.

The strains of *C. parapsilosis* were suspended in a saline solution and distributed on plates. After this process, the five discs (described above) were placed on plates containing the yeasts and incubated for 24 h at 35°C .

Association activity of miconazole with AgNPs could be calculated based on the inhibition zone on the agar using the formula: $((B^2 - A^2)/A^2)$, where A and B are the inhibition zones of miconazole alone and miconazole associated with AgNPs, respectively. In the absence of fungal growth, the disc size (22 mm) was used to calculate the increase in area. Furthermore, the increase in the calculated area was considered a synergy effect. At the same time, no change was characterized as indifferent, and the decrease in size was described as an antagonism between the components (da Frota et al. 2018).

Results and discussion

The synthesis conducted in this study involved the reduction of silver ions by glucose in an alkaline medium containing SDS in different concentrations. It is well-known that glucose reduces the silver ions to metallic silver through a glycolic acid oxidation process. Thus, since NaOH acts by opening the glucose molecule ring with its consecutive oxidation, it can accelerate the reduction of silver ions (Swenson et al. 2018). In addition, NaOH also leads to the formation of silver oxide, which facilitates the formation of silver zero-valent. After the first Ag^0 nuclei appear, the growth and stabilization of the silver nanoparticles are controlled by the diffusion and the attachment rates of SDS to the surface of the silver nanoparticles. Thus, the precipitation of the system containing 0.01 g of SDS (as shown in Fig. 1) indicates that only a tiny amount of surfactant is insufficient to control the growth and stabilize the silver nanoparticles. The samples synthesized using 0.25 and 0.50 g of SDS were stable in aqueous medium systems, indicating that the stabilization of the AgNPs occurs when the molar ratio Ag^+/SDS is less than 2.88. The reaction is represented in Fig. 1.

The yellow-colored AgNPs solution exhibited a localized surface plasmon resonance (LSPR) band centered around 420 nm (Fig. 2a). This band indicates the AgNPs formation since LSPR occurred due to interaction between the permanent dipole on the AgNPs surface and electromagnetic waves. The profile of LSPR also provides information about the homogeneity of the dispersion (Alula et al. 2018). Thus, as observed in Fig. 2a, the AgNPs-0.25 and AgNPs-0.50 samples have a UV–vis absorption band centered around 420 nm. For AgNPs-0.25, the wide UV–vis absorption band indicates heterogeneously dispersed AgNPs. Whereas for AgNPs-0.50, the profile suggests a narrow monodisperse

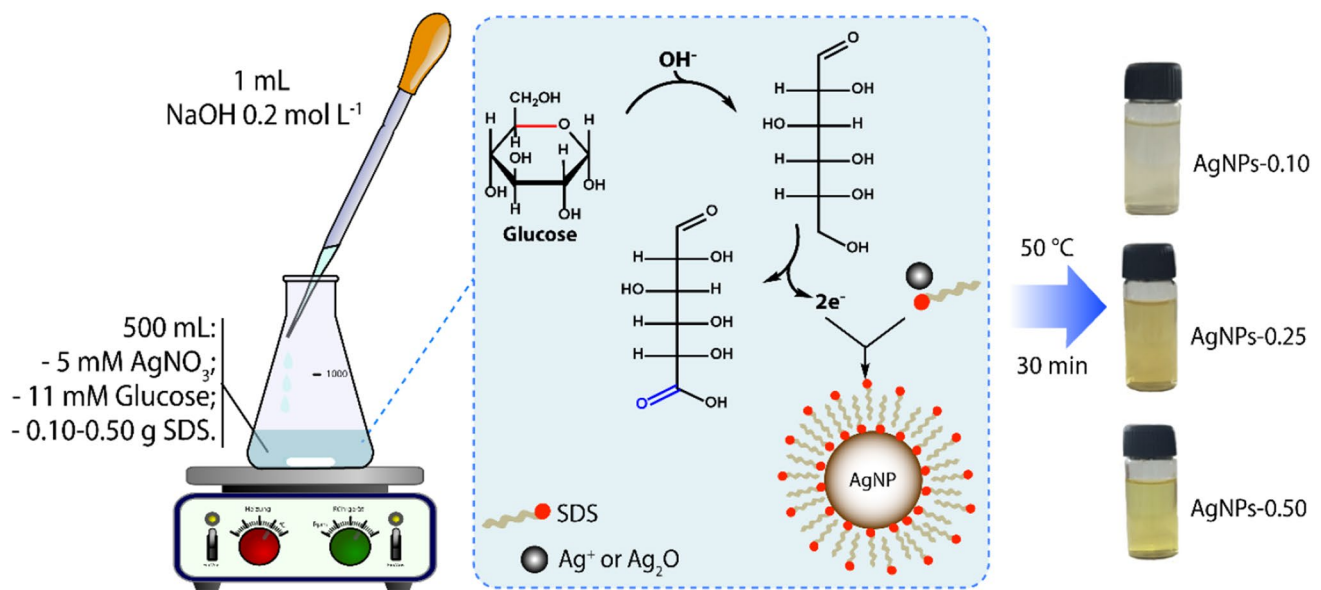


Fig. 1 Protocol of AgNPs synthesis using sugar as reduction agent and different amounts of SDS

population of silver nanoparticles. In addition, for the AgNPs-0.25 sample, a lower absorbance was also observed, evidencing a lower production and stabilization of AgNPs. Therefore, the lower amount of SDS was a determining factor for the lower stabilization rate of the nanoparticles (AgNPs-0.10).

FT-IR evaluates the interaction between AgNPs and their stabilizing agent (Fig. 2b). In the samples, bands of around 2908, 1151, and 1011 cm^{-1} can be assigned to $\nu_{\text{C-H}}$ of $-\text{CH}_2-$ groups and ν_{asym} and ν_{sym} of $-\text{SO}_3-$ groups, respectively (Rezaei et al. 2020). These bands suggest that SDS have been effectively adsorbed on the surface of the AgNPs. The wide band of 3330 cm^{-1} refers to the hydroxyl groups, which may be derived from glucose oxidation products adsorbed onto the AgNPs surface, SDS, NaOH or absorbed moisture (Kumar et al. 2012). There were no significant changes in the FTIR spectra for both synthesized samples, indicating that the coating was effective for both nanoparticles. To analyze the interaction of sulfate groups with nanoparticles surface, which can occur via different ways (monodentate; bidentate; bridging bidentate; ion interactions), the wave number separation, Δ , between ν_{asym} and ν_{sym} ($-\text{SO}_3-$) stretches were used. In the literature, it is reported that monodentate, bidentate and bridging dentate present Δ values around $< 110 \text{ cm}^{-1}$, 200–320 cm^{-1} and 140–190 cm^{-1} , respectively (Mehta et al. 2010). In this work, a Δ value around 140 cm^{-1} was observed, suggesting the formation of a bidentate complex on the AgNPs surface.

The hydrodynamic properties of aqueous AgNPs suspensions were studied using DLS measurements. The particle size distribution curves for the AgNPs-0.25 and AgNPs-0.50

samples are shown in Fig. 2c. The hydrodynamic size of AgNPs-0.5 was $77.58 \pm 47.08 \text{ nm}$ (mean \pm standard deviation), and the PDI (polydispersity index) was 0.189. International Standards Organization (ISOs) established that monodisperse particles must have a value of $\text{PDI} < 0.05$. However, it has been reported that silver colloidal systems with PDI values below 0.3 are acceptable and can be classified as narrow disperse systems (Sarkar et al. 2021; Wei et al. 2020). Therefore, this result is in accordance with the results obtained by UV-Vis spectroscopy, which presented a relatively wide half-maximum size (Cunha et al. 2018; Mehta et al. 2010). The AgNPs-0.25 sample had an average particle size of $91.22 \pm 29.37 \text{ nm}$ and a PDI of 0.225. The small amount of SDS in the synthesis of this sample (0.25 g) provided a weaker barrier to the nanoparticles growth, which resulted in a higher PDI value (0.225). Furthermore, the lower stabilizing electrostatic repulsion between the nanoparticles, due to the lower amount of SDS on the AgNPs surface, leads to cluster formation and a consequent broadening of the size distribution curve, as observed in Fig. 2c.

The zeta potential (ζ) is another important property related to the colloidal stability of the nanoparticles since it can estimate the surface charge magnitude related to particle stabilization. As shown in Fig. 2d, the ζ values for the AgNP-0.50 and AgNP-0.25 samples were -49.2 and -47.2 mV , respectively, which are above the estimated minimum ($\pm 30 \text{ mV}$) to provide enough electrostatic repulsion to counteract aggregation (Bélteky et al. 2021). In these systems, the surface charges are supplied by the sulfate groups of SDS, which are negatively charged. The slightly lower absolute value obtained for the AgNPs-0.25 sample is

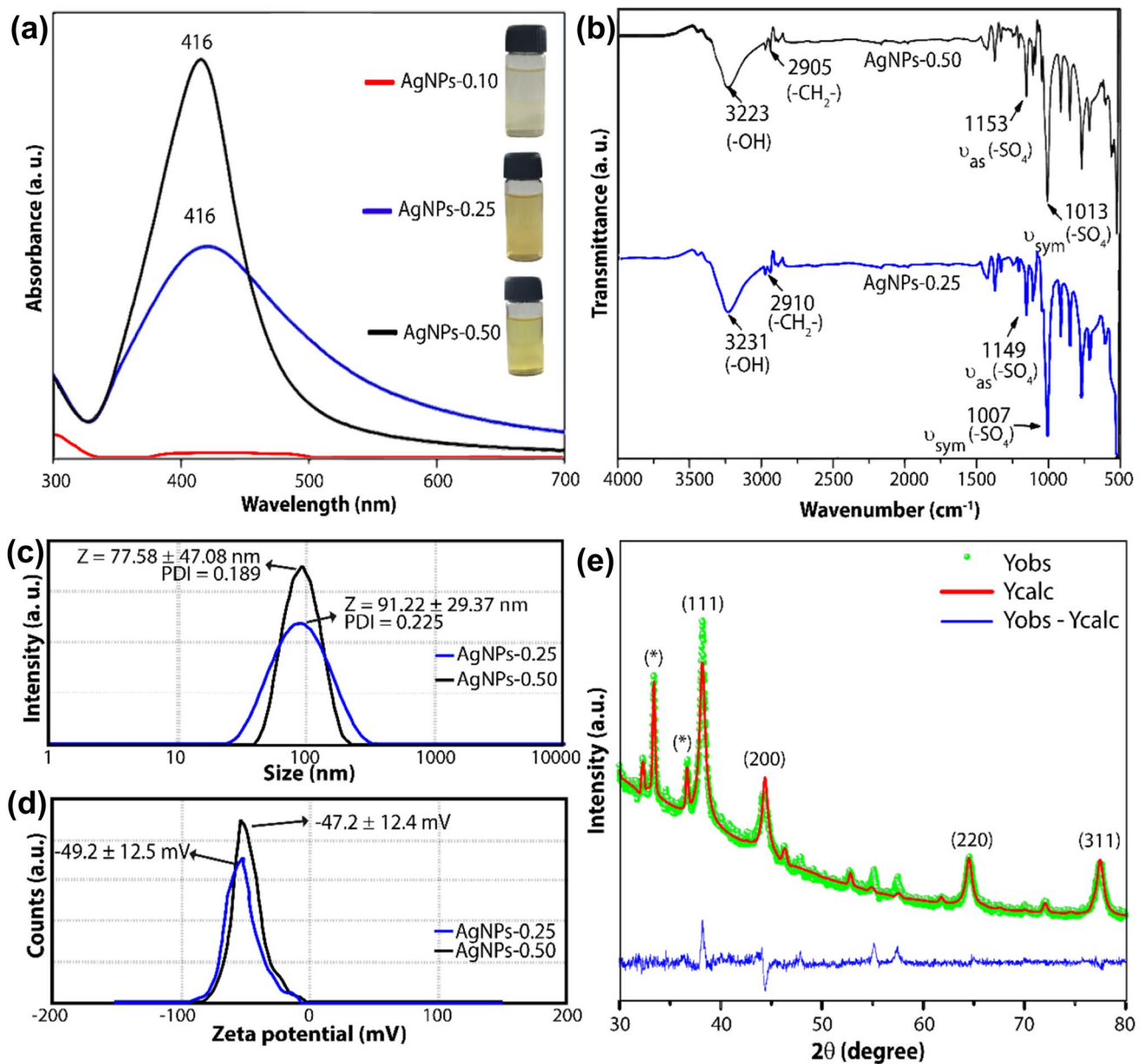


Fig. 2 Characterization of AgNPs: **a** UV–Visible spectra for the AgNPs suspensions; **b** FTIR spectra for dried AgNPs-0.25 (blue) and AgNPs-0.50 (black) samples; **c** Size and PDI, and **d** zeta potential

measurements for AgNPs-0.25 (blue) and AgNPs-0.50 (black); and **e** X-ray powder diffractogram for the AgNPs-0.50 sample

related to a smaller amount of SDS molecules on the surface of the silver nanoparticles. The ζ values found for both silver dispersion suggested excellent colloidal stability, indicating that the shelf life of the cream produced with these nanocomposites can be long time. It is worth emphasizing that the samples remained at room temperature (25 °C) and were not light-protected for at least three months before the DLS and (ζ) analysis.

To further confirm the structure of the metallic Ag phase formed, an XRD analysis was performed. Figure 2e shows the diffraction pattern for AgNP-0.50. The peaks

at 38.2°, 44.4°, 64.6° and 77.5° 2θ can be assigned to the planes (111), (200), (220), and (311) of the crystalline Ag phase with a face-centered cubic structure (JCPDS-087-0720), respectively (Soliman et al. 2021). This confirmation also can be observed from the refinement of the XRD pattern by the Rietveld method. In addition, other peaks were identified in the diffractogram, which can be assigned to the silver phosphate and the silver chloride phases. However, other works showed that these secondary phases did not influence microbiotic activity (Chandrasekharan

et al. 2022; Chudobova et al. 2013; Gordienko et al. 2019; Soliman et al. 2021).

SEM analyses were also performed to investigate the morphology of these nanoparticles, and the obtained data are shown in Fig. 3a–d. AgNP-0.25 and AgNP-0.50 samples have a spheroid structure and similar average particle size. This same morphology is also observed in other works (Sinha et al. 2012; Kora et al. 2009; Hamouda et al. 2019). However, also was noted that the clusters formed by AgNP-0.25 have a morphology more like a rod, while the clusters formed by AgNP-0.50 have a morphology spherical. This difference can be associated with less amount of SDS used during the synthesis process. As shown in the histograms (insets in Fig. 3a, b), the suspensions produced with 0.50 g SDS had an average particle size value of 92 ± 15 nm and a narrower size distribution, thereby in agreement with the results obtained by DLS. The AgNPs-0.25 samples are polydisperse, with particle size values ranging from 50 to 150 nm. As shown so far, AgNPs-0.50 suspension has higher stability and narrower dispersion than AgNP-0.25, thus,

more desirable for formulations such as the vaginal cream developed in this work. Figure 3e shows the EDX spectra for the AgNPs-0.50 sample, where the principal component is noticeably silver, which absorbs energy around 3 keV. Other elements in the spectra are related to excipients from the used precursors in the reaction. There was no significant difference in the morphology of the two synthesized AgNPs suspensions.

The antibiotic susceptibility test using the *C. parapsilosis*-strains is shown in Fig. 4. The increase of the inhibition area was calculated using the formula $(B^2 - A^2)/A^2$, where A and B are the inhibition zone diameters related to pure miconazole and miconazole associated with AgNPs, respectively. Figure 4a shows the inhibition zones caused by miconazole and AgNPs alone and their associations. An enhancement in fungal growth inhibition is evident when miconazole is combined with AgNPs. The average diameters of each zone as a function of three products, miconazole, miconazole + AgNPs-0.25, and miconazole + AgNPs-0.50 (Fig. 4b), as well as the increase in inhibition area compared to the

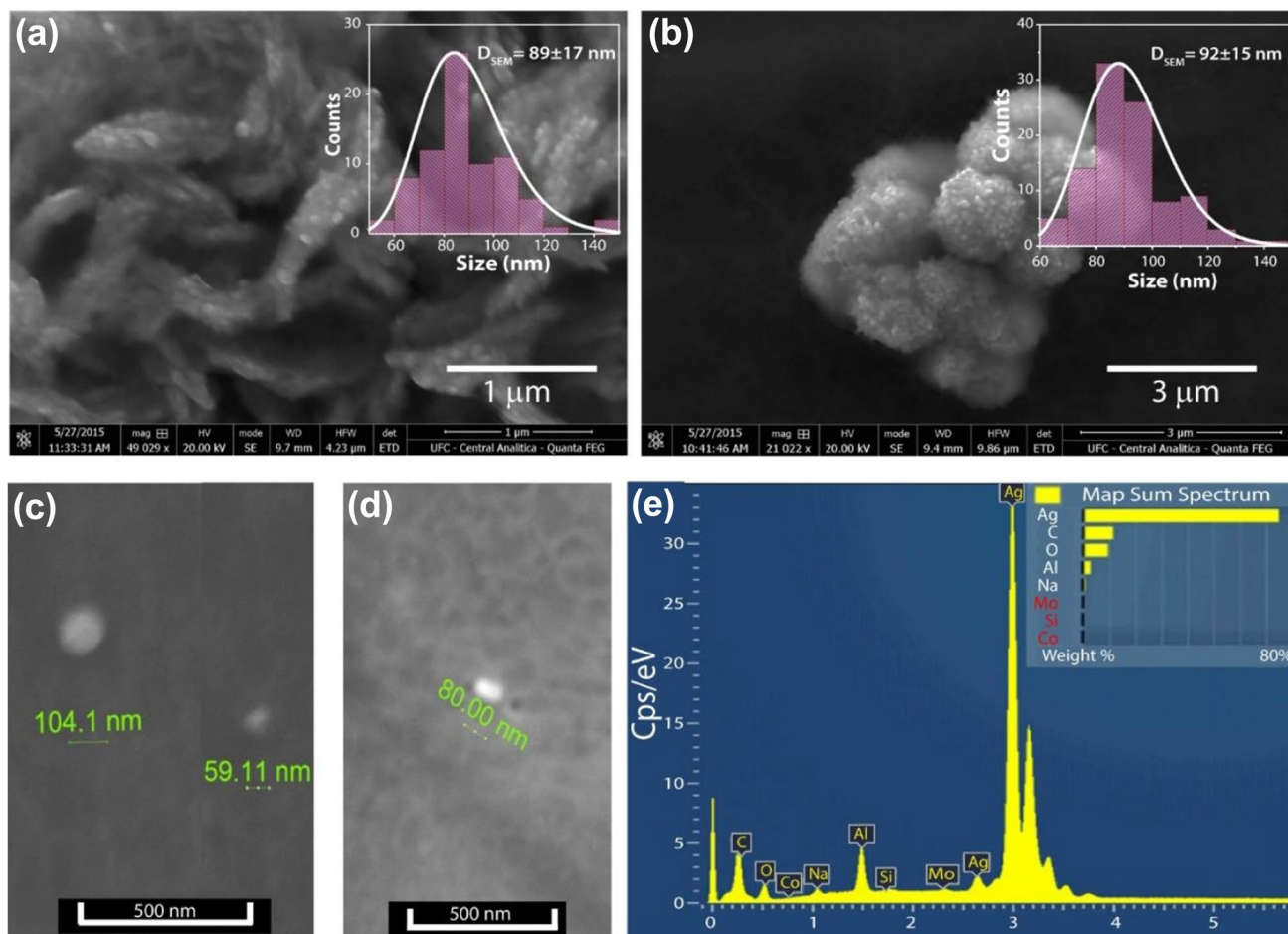


Fig. 3 SEM images of the AgNPs-0.25 (a, c) and AgNPs-0.50 (b, d); e Energy dispersive X-ray Spectroscopy (EDS) spectra of AgNP-0.50 sample

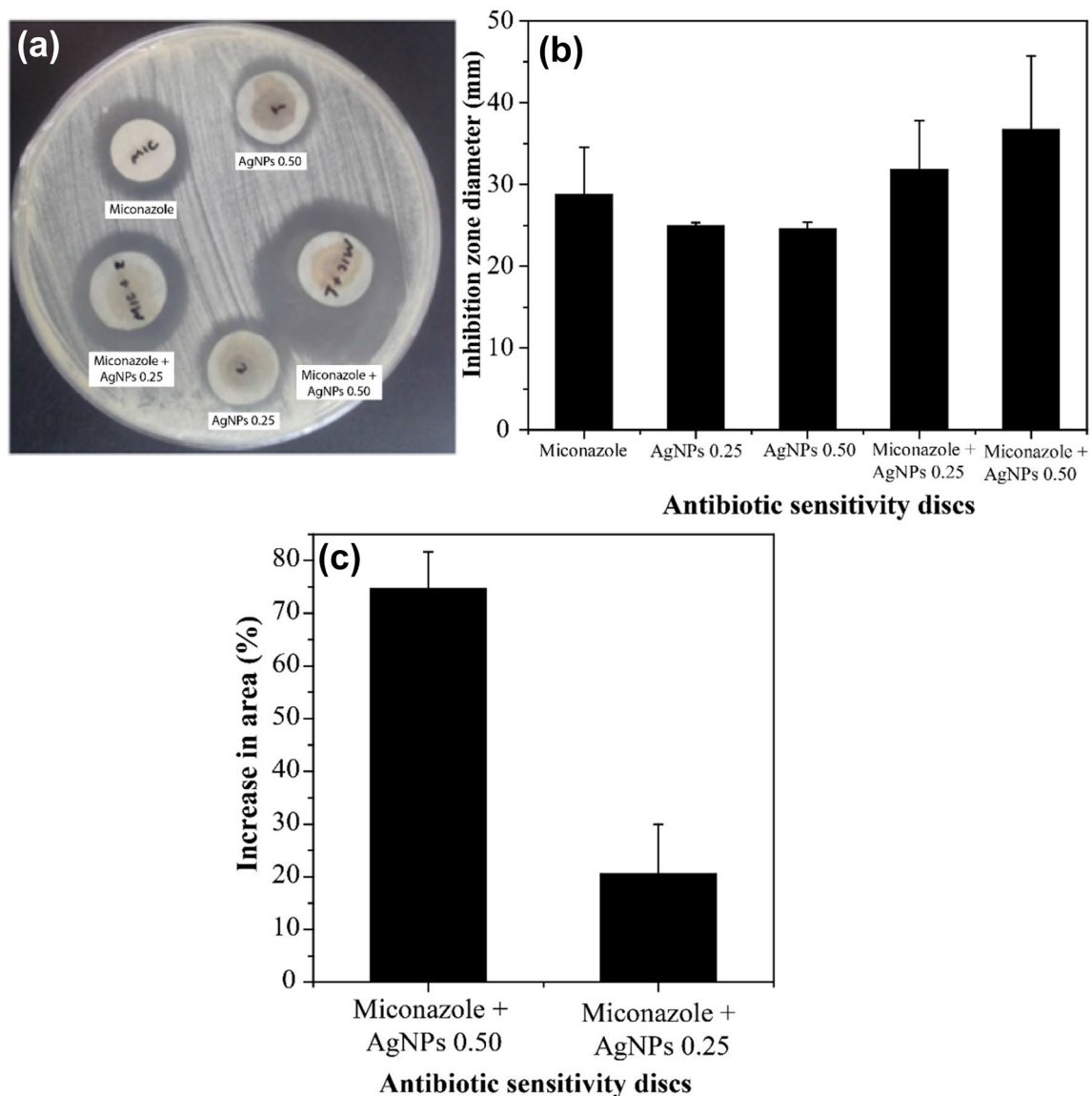


Fig. 4 Sensitivity test with *C. parapsilosis*: **a** Inhibition zones caused by isolated miconazole, AgNPs and their association; **b** comparison of the mean inhibition zone diameter for miconazole 25 μ g and its association with AgNPs-0.25 and AgNPs-0.50 suspensions; **c** com-

parison of the synergic effect (through the increase in area percentage) between miconazole and the AgNPs-0.25 and AgNPs-0.50 suspensions

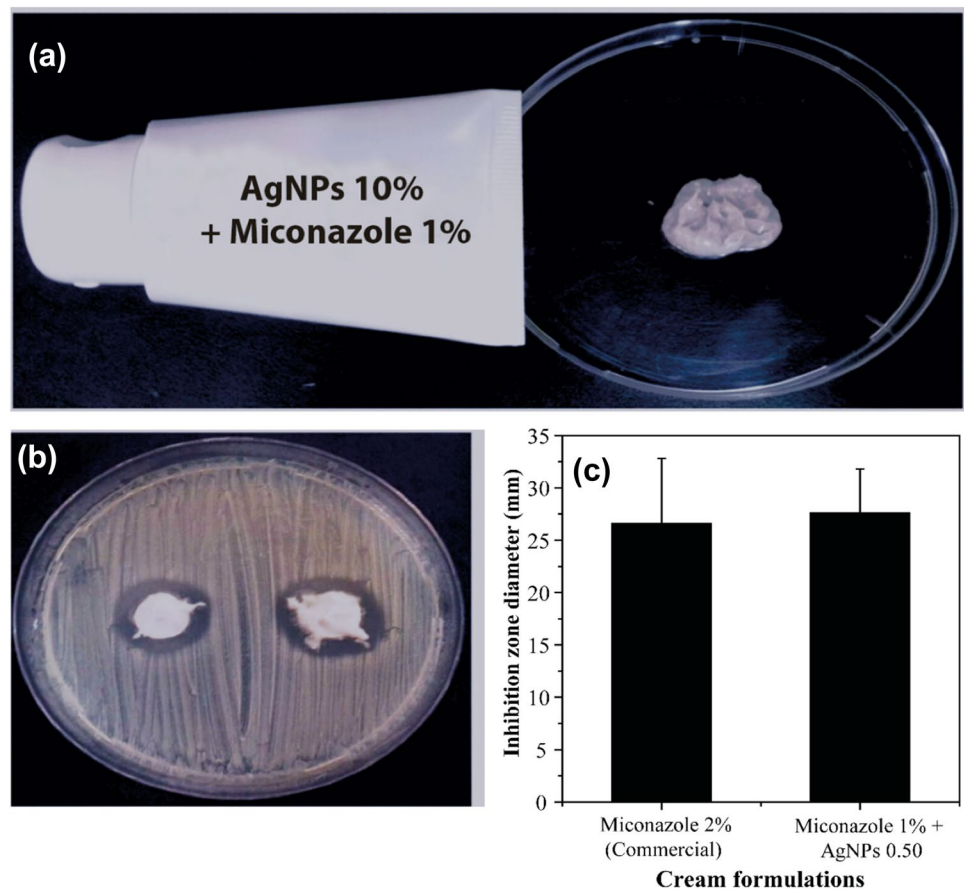
reference (miconazole) (Fig. 4c), were compared. Again, a synergistic effect between the two agents was observed. The AgNPs-0.50 suspension performed better since the SDS coating enabled more AgNPs to be suspended in the final product. The results showed that AgNPs are stable and have activity against *C. parapsilosis*. The next step of the work was the preparation of an anti-candida cream that combines miconazole and AgNPs.

AgNPs-0.50 was the sample chosen to produce the cream because it had better dispersion, colloidal stability and antifungal activity when associated with miconazole. Therefore, a cream based on this combination was developed

(Fig. 5a) to evaluate its antimicrobial effect on *C. parapsilosis* (Fig. 5b). Carbopol was used as the vehicle because of its gelling and bioadhesion properties, which are suitable for application in the vagina, as well as its ability to deliver the drug in a controlled way (Tayah and Eid 2023; Salah et al. 2018; Patil et al. 2022).

The approach of our formulation is in line with the established strategies outlined in the work of Kumar and Poornachandra, which used AgNPs as a carrier for miconazole, achieving a controlled release for up to 6 h (Kumar and Poornachandra 2015). In addition, Salah, Awad and Makhoul have shown that carbopol can delay the release

Fig. 5 **a** Anti-candida cream made with miconazole and silver nanoparticles; **b** view of the petri dish containing the cream and *C. parapsilosis* **c** comparison of the inhibition zone diameter derived from the cream synthesized in this work and a record market



of drugs by carrier systems such as Eugragit® RS 100. Furthermore, the authors provided insights into the mechanisms behind the sustained release behavior observed in similar gel formulations (Salah et al. 2018). Therefore, there is reason to believe that the combination of AgNPs-0.50 with miconazole and Carbopol will increase therapeutic efficacy by releasing this drug in a controlled way, avoiding resistance mechanisms.

The obtained cream was compared to a commercial cream with 2% miconazole (Fig. 5c) and proved very suitable since it increased the average diameter of the inhibition zone. It is important to record that the formulation development in this work has a 50% smaller quantity of miconazole. In addition, despite the dark coloration of the AgNPs, the prototype cream had a light-colored appearance, which makes it acceptable for marketing. Although further studies must be performed, the herein-prepared cream proved promising due to its evident antifungal effect.

It is essential to consider the safety implications of using AgNPs in biomedical applications. Several factors contribute to the toxicity of AgNPs, including their size, surface charge, surface chemistry, and concentration. At higher concentrations, AgNPs can induce cytotoxicity by causing oxidative stress, DNA damage, and cellular apoptosis (Jian

et al. 2022). The specific dosage at which AgNPs exhibit toxicity can vary between different cell types, experimental conditions, and exposure durations (Mondal et al. 2020; AlJindan and AlEraky 2022). They can also interfere with cellular processes and disrupt the normal functioning of organelles (Radhakrishnan et al. 2018).

Conclusion

AgNPs were easily obtained through a simple and environmentally friendly method and characterized by UV–Vis, FT-IR, XRD, and EDX analysis. The AgNPs produced were stable and monodisperse (AgNP-0.25 and AgNP-0.50), showing activity against *C. parapsilosis* when isolated or in combination with miconazole. The formulation of the cream was easy to perform [miconazole (1%) + AgNP-0.50 (10%)]. The results of the cream were also satisfactory, considering the 50% reduction of the concentration of miconazole compared to the concentration in a cream already registered on the market and still having larger inhibition zones.

Considering the potential toxicity associated with AgNPs, it is crucial to strike a balance between their antimicrobial efficacy and safety. Future research should aim to optimize

the concentration and formulation of AgNPs to minimize potential adverse effects while maximizing their therapeutic benefits in the treatment of Vulvovaginal Candidiasis (VVC) and Recurrent Vulvovaginal Candidiasis (RVVC). The potential toxic effects of AgNPs at the concentration used in this study should be carefully considered and thoroughly investigated. Understanding the biocompatibility and safety profile of AgNPs is crucial for their successful translation into clinical applications.

Acknowledgements The authors thank Central Analítica-UFC/CT-INFRA/MCTI-SISNANO/Pró-Equipamentos for providing the SEM experiments and X-ray Diffraction Laboratory (LRX-UFC). This work was partially supported by NanoSaude: E-26/010.000981/2019, UEZO: E-26/010.002362/2019; Temáticos: E-26/211.269/2021, Infraestrutura and Pesquisa na UEZO, UERJ: E-26/211.207/2021, Bolsa de Pós-Doutorado Senior (PDS): E-26/202.320/2021 and CNPq (Bolsa de Produtividade 1C: 308452/2022-4 and 1B: 301069/2018-2). This work was also supported by CAPES (Finance Code 001-PROEX 23038.000509/2020-82) and Funcap (PNE-0112-00048.01.00/16).

Data availability Not applicable.

Declarations

Conflict of interest The authors have no relevant financial or non-financial interests to disclose.

Ethical approval This study did not involve the use of any human or animal model.

Informed consent Not applicable.


References

- Al-Bahrani RM, Majeed SMA, Owaid MN, Mohammed AB, Rheem DAJAPS (2018) Phyto-fabrication, characteristics and anticandidal effects of silver nanoparticles from leaves of *Ziziphus mauritiana* Lam. *ACTA Pharm Sci* 56(3):85
- AlJindan R, AlEraky DM (2022) Silver nanoparticles: a promising antifungal agent against the growth and biofilm formation of the emergent *Candida auris*. *J Fungi (basel)* 8(7):744. <https://doi.org/10.3390/jof8070744>
- Alula MT, Karamchand L, Hendricks NR, Blackburn JM (2018) Citrate-capped silver nanoparticles as a probe for sensitive and selective colorimetric and spectrophotometric sensing of creatinine in human urine. *Anal Chim Acta* 1007:40–49. <https://doi.org/10.1016/j.aca.2017.12.016>
- Bélteky P, Rónavári A, Zakupszky D, Boka E, Igaz N, Szerencsés B, Pfeiffer I, Vágvolgyi C, Kiricsi M, Kónya Z (2021) Are smaller nanoparticles always better? Understanding the biological effect of size-dependent silver nanoparticle aggregation under biorelevant conditions. *Int J Nanomed* 16:3021–3040. <https://doi.org/10.2147/IJN.S304138>
- Chandrasekharan S, Chinnasamy G, Bhatnagar S (2022) Sustainable phyto-fabrication of silver nanoparticles using *Gmelina arborea* exhibit antimicrobial and biofilm inhibition activity. *Sci Rep* 12(1):156. <https://doi.org/10.1038/s41598-021-04025-w>
- Chudobova D, Nejdil L, Gumulec J, Krystofova O, Rodrigo MA, Kynicky J, Ruttkay-Nedecky B, Kopel P, Babula P, Adam V, Kizek R (2013) Complexes of silver(I) ions and silver phosphate nanoparticles with hyaluronic acid and/or chitosan as promising antimicrobial agents for vascular grafts. *Int J Mol Sci* 14(7):13592–13614. <https://doi.org/10.3390/ijms140713592>
- Cianci A, Cicinelli E, Colacurci N, De Leo V, Perino A, Pino A, Bartolo E, Randazzo C, Esposito G, Chiaffarino F (2020) Diagnosis and treatment of vulvovaginal candidiasis: a practical approach. *Ital J Gynaecol Obstetr* 32(4):261–268
- Cunha FA, Cunha M, da Frota SM, Mallmann EJJ, Freire TM, Costa LS, Paula AJ, Menezes EA, Fechine PBA (2018) Biogenic synthesis of multifunctional silver nanoparticles from *Rhodotorula glutinis* and *Rhodotorula mucilaginosa*: antifungal, catalytic and cytotoxicity activities. *World J Microbiol Biotechnol* 34(9):127. <https://doi.org/10.1007/s11274-018-2514-8>
- da Frota S, Cunha F, Cunha MR, Menezes EJ (2018) synergistic effect of polyene antifungals and silver nanoparticles against *Candida parapsilosis*. *J Antibiot Res* 2(1):104
- Devi LS, Joshi SR (2012) Antimicrobial and synergistic effects of silver nanoparticles synthesized using soil fungi of high altitudes of eastern Himalaya. *Mycobiology* 40(1):27–34. <https://doi.org/10.5941/MYCO.2012.40.1.027>
- Dhasarathan P, AlSalhi MS, Devanesan S, Subbiah J, Ranjitsingh AJA, Binsalah M, Alfuraydi AA (2021) Drug resistance in *Candida albicans* isolates and related changes in the structural domain of Mdr1 protein. *J Infect Public Health* 14(12):1848–1853. <https://doi.org/10.1016/j.jiph.2021.11.002>
- Farr A, Effendy I, Frey Tirri B, Hof H, Maysen P, Petricevic L, Ruhnke M, Schaller M, Schaefer APA, Sustr V, Willinger B, Mendling W (2021) Guideline: vulvovaginal candidosis (AWMF 015/072, level S2k). *Mycoses* 64(6):583–602. <https://doi.org/10.1111/myc.13248>
- Gordienko MG, Palchikova VV, Kalenov SV, Belov AA, Lyasnikova VN, Poberezhniy DY, Chibisova AV, Sorokin VV, Skladnev DA (2019) Antimicrobial activity of silver salt and silver nanoparticles in different forms against microorganisms of different taxonomic groups. *J Hazard Mater* 378:120754. <https://doi.org/10.1016/j.jhazmat.2019.120754>
- Guerra JD, Sandoval G, Avalos-Borja M, Pestryakov A, Garibo D, Susarrey-Arce A, Bogdanchikova N (2020) Selective antifungal activity of silver nanoparticles: a comparative study between *Candida tropicalis* and *Saccharomyces boulardii*. *Colloid Interface Sci Commun* 37:100280. <https://doi.org/10.1016/j.colcom.2020.100280>
- Hamouda RA, Abd El-Mongy M, Eid KF (2019) Comparative study between two red algae for biosynthesis silver nanoparticles capping by SDS: insights of characterization and antibacterial activity. *Microb Pathog* 129:224–232. <https://doi.org/10.1016/j.micpath.2019.02.016>
- Hashemi Z, Mizwari ZM, Mohammadi-Aghdam S, Mortazavi-Derazkola S, Ali Ebrahimzadeh M (2022) Sustainable green synthesis of silver nanoparticles using *Sambucus ebulus* phenolic extract (AgNPs@SEE): optimization and assessment of photocatalytic degradation of methyl orange and their in vitro antibacterial and anticancer activity. *Arab J Chem* 15(1):103525. <https://doi.org/10.1016/j.arabj.2021.103525>
- Jian Y, Chen X, Ahmed T, Shang Q, Zhang S, Ma Z, Yin Y (2022) Toxicity and action mechanisms of silver nanoparticles against the mycotoxin-producing fungus *Fusarium graminearum*. *J Adv Res* 38:1–12. <https://doi.org/10.1016/j.jare.2021.09.006>
- Johnson MD (2021) Antifungals in clinical use and the pipeline. *Infect Dis Clin North Am* 35(2):341–371. <https://doi.org/10.1016/j.idc.2021.03.005>
- Kora AJ, Manjusha R, Arunachalam J (2009) Superior bactericidal activity of SDS capped silver nanoparticles: synthesis and characterization. *Mater Sci Eng C* 29(7):2104–2109. <https://doi.org/10.1016/j.msec.2009.04.010>
- Kumar CG, Poornachandra Y (2015) Biodirected synthesis of Miconazole-conjugated bacterial silver nanoparticles and their application

- as antifungal agents and drug delivery vehicles. *Colloids Surf B* 125:110–119. <https://doi.org/10.1016/j.colsurfb.2014.11.025>
- Kumar CG, Mamidyalala SK, Reddy MN, Reddy BVS (2012) Silver glyconanoparticles functionalized with sugars of sweet sorghum syrup as an antimicrobial agent. *Process Biochem* 47(10):1488–1495. <https://doi.org/10.1016/j.procbio.2012.05.023>
- Lírio J, Giraldo PC, Sarmiento AC, Costa APF, Cobucci RN, Saconato H, Eleutério Júnior J, Gonçalves AK (2022) Antifungal (oral and vaginal) therapy for recurrent vulvovaginal candidiasis: a systematic review and meta-analysis. *Rev Assoc Med Brasil* (1992) 68(2):261–267. <https://doi.org/10.1590/1806-9282.20210916>
- Mare AD, Man A, Ciurea CN, Toma F, Cighir A, Mareş M, Berta L, Tanase C (2021) Silver nanoparticles biosynthesized with spruce bark extract—a molecular aggregate with antifungal activity against *Candida* species. *Antibiotics* 10(10):1261
- Mehta SK, Chaudhary S, Gradzielski M (2010) Time dependence of nucleation and growth of silver nanoparticles generated by sugar reduction in micellar media. *J Colloid Interface Sci* 343(2):447–453. <https://doi.org/10.1016/j.jcis.2009.11.053>
- Menezes EA, Vasconcelos Júnior AAd, Cunha FA, Cunha MCdSO, Braz BHL, Capelo LG, Silva CLF (2012) Molecular identification and antifungal susceptibility of *Candida parapsilosis* isolates in Ceará, Brazil. *J Bras Patol Med Lab* 48:415–420
- Mondal AH, Yadav D, Ali A, Khan N, Jin JO, Haq QMR (2020) Anti-bacterial and anti-candidal activity of silver nanoparticles biosynthesized using *Citrobacter* spp. MS5 culture supernatant. *Biomolecules* 10(6):944. <https://doi.org/10.3390/biom10060944>
- Moshfeghy Z, Tahari S, Janghorban R, Najib FS, Mani A, Sayadi M (2020) Association of sexual function and psychological symptoms including depression, anxiety and stress in women with recurrent vulvovaginal candidiasis. *J Turk German Gynecol Assoc* 21(2):90–96. <https://doi.org/10.4274/jtggg.galenos.2019.2019.0077>
- Panáček A, Kolář M, Večeřová R, Pucek R, Soukupová J, Kryštof V, Hamal P, Zbořil R, Kvítek L (2009) Antifungal activity of silver nanoparticles against *Candida* spp. *Biomaterials* 30(31):6333–6340. <https://doi.org/10.1016/j.biomaterials.2009.07.065>
- Parsapour H, Masoumi SZ, Shayan A, Moradkhani S, Ghiasian SA, Rashidi MK (2021) Comparison of the effects of nika vaginal cream with clotrimazole cream on vaginal candidiasis symptoms: A randomized single-blind clinical trial. *Iran J Nurs Midwifery Res* 26(6):521–525. https://doi.org/10.4103/ijnmr.IJNMR_82_20
- Patil MU, Rajput AP, Belgamwar VS, Chalikwar SS (2022) Development and characterization of amphotericin B nanoemulsion-loaded mucoadhesive gel for treatment of vulvovaginal candidiasis. *Heliyon* 8(11):e11489. <https://doi.org/10.1016/j.heliyon.2022.e11489>
- Radhakrishnan VS, Reddy Mudiam MK, Kumar M, Dwivedi SP, Singh SP, Prasad T (2018) Silver nanoparticles induced alterations in multiple cellular targets, which are critical for drug susceptibilities and pathogenicity in fungal pathogen (*Candida albicans*). *Int J Nanomedicine* 13:2647–2663. <https://doi.org/10.2147/ijn.S150648>
- Rezaei H, Rahimpour E, Khoubnasabjafari M, Jouyban-Gharamaleki V, Jouyban A (2020) A colorimetric nanoprobe based on dynamic aggregation of SDS-capped silver nanoparticles for tobramycin determination in exhaled breath condensate. *Microchim Acta* 187(3):186. <https://doi.org/10.1007/s00604-020-4162-6>
- Rosati D, Bruno M, Jaeger M, Ten Oever J, Netea MG (2020) Recurrent vulvovaginal candidiasis: an immunological perspective. *Microorganisms* 8(2):144. <https://doi.org/10.3390/microorgan8020144>
- Salah S, Awad GEA, Makhlof AIA (2018) Improved vaginal retention and enhanced antifungal activity of miconazole microsponges gel: formulation development and in vivo therapeutic efficacy in rats. *Eur J Pharm Sci* 114:255–266. <https://doi.org/10.1016/j.ejps.2017.12.023>
- Sarkar M, Denrah S, Das M, Das M (2021) Statistical optimization of bio-mediated silver nanoparticles synthesis for use in catalytic degradation of some azo dyes. *Chem Phys Impact* 3:100053. <https://doi.org/10.1016/j.chphi.2021.100053>
- Singh M, Kumar M, Kalaivani R, Manikandan S, Kumaraguru AK (2013) Metallic silver nanoparticle: a therapeutic agent in combination with antifungal drug against human fungal pathogen. *Bioprocess Biosyst Eng* 36(4):407–415. <https://doi.org/10.1007/s00449-012-0797-y>
- Sinha T, Gude V, Rao NVS (2012) Synthesis of silver nanoparticles using sodium dodecylsulphate. *Adv Sci Eng Med* 4(5):381–387. <https://doi.org/10.1166/asem.2012.1195>
- Sobel JD, Nyirjesy P (2021) Oteseconazole: an advance in treatment of recurrent vulvovaginal candidiasis. *Future Microbiol* 16(18):1453–1461. <https://doi.org/10.2217/fmb-2021-0173>
- Soliman AM, Abdel-Latif W, Shehata IH, Fouda A, Abdo AM, Ahmed YM (2021) Green approach to overcome the resistance pattern of *Candida* spp. using biosynthesized silver nanoparticles fabricated by *Penicillium chrysogenum* F9. *Biol Trace Elem Res* 199(2):800–811. <https://doi.org/10.1007/s12011-020-02188-7>
- Swensson B, Ek M, Gray DG (2018) In situ preparation of silver nanoparticles in paper by reduction with alkaline glucose solutions. *ACS Omega* 3(8):9449–9452. <https://doi.org/10.1021/acsomega.8b01199>
- Szerencsés B, Igaz N, Tóbiás Á, Prucsi Z, Rónavári A, Béteky P, Madarász D, Papp C, Makra I, Vágvolgyi C, Kónya Z, Pfeiffer I, Kiricsi M (2020) Size-dependent activity of silver nanoparticles on the morphological switch and biofilm formation of opportunistic pathogenic yeasts. *BMC Microbiol* 20(1):176. <https://doi.org/10.1186/s12866-020-01858-9>
- Tauseef A, Hisam F, Hussain T, Caruso A, Hussain K, Châtel A, Chénais B (2022) Nanomicrobiology: emerging trends in microbial synthesis of nanomaterials and their applications. *J Cluster Sci*. <https://doi.org/10.1007/s10876-022-02256-z>
- Tayah DY, Eid AM (2023) Development of miconazole nitrate nanoparticles loaded in nanoemulgel to improve its antifungal activity. *Saudi Pharm J* 31(4):526–534. <https://doi.org/10.1016/j.jsps.2023.02.005>
- Tóth R, Nosek J, Mora-Montes HM, Gabaldon T, Bliss JM, Nosanchuk JD, Turner SA, Butler G, Vágvolgyi C, Gácsér A (2019) *Candida parapsilosis*: from genes to the bedside. *Clin Microbiol Rev*. <https://doi.org/10.1128/cmr.00111-18>
- Vazquez-Muñoz R, Avalos-Borja M, Castro-Longoria E (2014) Ultrastructural analysis of *Candida albicans* when exposed to silver nanoparticles. *PLoS ONE* 9(10):e108876. <https://doi.org/10.1371/journal.pone.0108876>
- Wei S, Wang Y, Tang Z, Hu J, Su R, Lin J, Zhou T, Guo H, Wang N, Xu R (2020) A size-controlled green synthesis of silver nanoparticles by using the berry extract of Sea Buckthorn and their biological activities. *New J Chem* 44(22):9304–9312. <https://doi.org/10.1039/D0NJ01335H>
- Willems HME, Ahmed SS, Liu J, Xu Z, Peters BM (2020) Vulvovaginal candidiasis: a current understanding and burning questions. *J Fungi (basel)* 6(1):27. <https://doi.org/10.3390/jof6010027>

Springer Nature or its licensor (e.g. a society or other partner) holds exclusive rights to this article under a publishing agreement with the author(s) or other rightsholder(s); author self-archiving of the accepted manuscript version of this article is solely governed by the terms of such publishing agreement and applicable law.

Authors and Affiliations

Antônio Auberson Martins Maciel^{1,2} · Francisco Afrânio Cunha^{1,2} · Tiago Melo Freire¹ · Fernando Lima de Menezes¹ · Lillian Maria Uchoa Dutra Fechine¹ · Janaina Sobreira Rocha¹ · Rita de Cássia Carvalho Barbosa² · Roxeane Teles Martins² · Maria da Conceição dos Santos Oliveira Cunha^{3,4} · Ralph Santos-Oliveira^{5,6} · Maria Veraci Oliveira Queiroz³ · Pierre Basílio Almeida Fechine¹ 

✉ Pierre Basílio Almeida Fechine
fechine@ufc.br

Antônio Auberson Martins Maciel
aubersonfarmaufc@gmail.com

Francisco Afrânio Cunha
afranio@ufc.br

Tiago Melo Freire
tiagomf@ufc.br

Fernando Lima de Menezes
fdolime@gmail.com

Lillian Maria Uchoa Dutra Fechine
lmudutra@hotmail.com

Janaina Sobreira Rocha
janaina.s@fisica.ufc.br

Rita de Cássia Carvalho Barbosa
ritacassiacb@yahoo.com.br

Roxeane Teles Martins
roxeanemartins@gmail.com

Maria da Conceição dos Santos Oliveira Cunha
cecinhya@gmail.com

Ralph Santos-Oliveira
roliveira@ien.gov.br

Maria Veraci Oliveira Queiroz
veracioq@hotmail.com

¹ Advanced Materials Chemistry Group (GQMat), Department of Analytical Chemistry and Physical Chemistry, Federal University of Ceará (UFC), Pici Campus, 12100, Fortaleza, CE 60451-970, Brazil

² Department of Clinical and Toxicological Analysis, Federal University of Ceará (UFC), Capitão Francisco Pedro Street, 1210, Rodolfo Teófilo, Fortaleza, CE 60270-430, Brazil

³ State University of Ceará. Graduate Program in Clinical Care in Nursing and Health, Fortaleza, CE, Brazil

⁴ Princesa do Oeste College, Crateús, CE, Brazil

⁵ Laboratory of Nanoradiopharmacy and Synthesis of New Radiopharmaceuticals, Brazilian Nuclear Energy Commission, Nuclear Engineering Institute, Rio de Janeiro, RJ 21941906, Brazil

⁶ Laboratory of Nanoradiopharmacy and Strategic Biomaterials, Zona Oeste State University, Rio de Janeiro, RJ 220000, Brazil